RL-TR-96-129
Final Technical Report
July 1996

OPTICAL WAVELET PREPROCESSING

Florida Institute of Technology

Samuel P. Kozaitis

APPROVED FOR PUBLIC RELEASE; DISTRIBUTION UNLIMITED.

Rome Laboratory
Air Force Materiel Command
Rome, New York

This report has been reviewed by the Rome Laboratory Public Affairs Office (PA) and is releasable to the National Technical Information Service (NTIS). At NTIS, it will be releasable to the general public, including foreign nations.

RL-TR- 96-129 has been reviewed and is approved for publication.

APPROVED: Mark A. Getbehead

MARK A. GETBEHEAD
Project Engineer

FOR THE COMMANDER: Gary D. Barmore

GARY D. BARMORE, Major, USAF
Deputy Director of Surveillance & Photonics

If your address has changed or if you wish to be removed from the Rome Laboratory mailing list, or if the addressee is no longer employed by your organization, please notify Rome Laboratory/ (OCPA), Rome NY 13441. This will assist us in maintaining a current mailing list.

Do not return copies of this report unless contractual obligations or notices on a specific document require that it be returned.

REPORT DOCUMENTATION PAGE

Form Approved
OMB No. 0704-0188

1. AGENCY USE ONLY (Leave Blank)	2. REPORT DATE	3. REPORT TYPE AND DATES COVERED
	July 1996	Final May 95 - Feb 96

4. TITLE AND SUBTITLE

OPTICAL WAVELET PREPROCESSING

5. FUNDING NUMBERS

C - F30602-95-C-0068
PE - 62702F
PR - 4600
TA - P4
WU - PM

6. AUTHOR(S)

Samuel P. Kozaitis

7. PERFORMING ORGANIZATION NAME(S) AND ADDRESS(ES)

Florida Institute of Technology
150 W. University Blvd.
Melbourne FL 32901-6988

8. PERFORMING ORGANIZATION REPORT NUMBER

N/A

9. SPONSORING/MONITORING AGENCY NAME(S) AND ADDRESS(ES)

Rome Laboratory/OCPA
25 Electronic Pky
Rome NY 13441-4515

10. SPONSORING/MONITORING AGENCY REPORT NUMBER

RL-TR-96-129

11. SUPPLEMENTARY NOTES

Rome Laboratory Project Engineer: Mark A. Getbehead/OCPA/(315) 330-4146

12a. DISTRIBUTION/AVAILABILITY STATEMENT

Approved for public release; distribution unlimited.

12b. DISTRIBUTION CODE

13. ABSTRACT (Maximum 200 words)

A low resolution image was used for object recognition using an optical correlation technique. The low resolution image was an approximation of the original image that was derived using a discrete wavelet transform. The low resolution image was cross-correlated with an image containing an object of interest. Using an inverse wavelet transform, the cross-correlation result was synthesized to the resolution of the original image. This approach avoids cross-correlating an image multiple times and passing information between levels of an image representation. It was shown that objects could be recognized that were approximated at 1/4 the original resolution using binary phase-only correlation filters. Discrimination decreased at the lower resolutions, but the technique looks useful for object recognition.

14. SUBJECT TERMS

Wavelet transform, Optical correlator, Low resolution correlation, Binary phase-only filters

15. NUMBER OF PAGES

28

16. PRICE CODE

17. SECURITY CLASSIFICATION OF REPORT	18. SECURITY CLASSIFICATION OF THIS PAGE	19. SECURITY CLASSIFICATION OF ABSTRACT	20. LIMITATION OF ABSTRACT
UNCLASSIFIED	UNCLASSIFIED	UNCLASSIFIED	UL

Table of Contents

Abstract

We used the discrete wavelet transform to approximate an image at a lower resolution as pre-processing for object recognition using an optical correlation technique. We cross-correlated the low-resolution image with a similarly processed image containing an object of interest. Then, we synthesized the cross-correlation result to the resolution of the original image. Using this approach, we avoided cross-correlating an image multiple times and passing information between levels of an image representation such as in a pyramid representation. We showed that we could recognize objects that were approximated at 1/4 the original resolution using binary phase-only correlation filters. Although discrimination decreased when compared to processing at the original resolution, it appeared that the results were useful for object recognition. We chose wavelets based on their impulse response of our system, and found that different wavelet filters gave different autocorrelation peak, and SNR values. Our study gave insight into the performance that may be expected when performing pattern recognition on images approximated by the wavelet transform.

1.0 Introduction

The application of optical correlators is often limited by the number of pixels in a spatial light modulator (SLM). Many applications require at least 512 x 512 pixels, which is larger than most SLMs, and applications requiring more pixels are common. One approach to this problem has been to process a large image at lower resolutions beginning with the lowest resolution. In this way, the image is decomposed into a pyramid representation.[1,2] A low-resolution version of an image may be used to find regions of interest in an image that gives only the approximate identity and location of a object. To determine these parameters more precisely, information must be passed from the lower-resolution version of the image to a higher-resolution version that is processed further. This procedure is repeated until the highest resolution of the pyramid is reached.

Because the resolution of a pixelated SLM is fixed, only a constant size image can be processed. Therefore, only a portion of an image can be processed as its resolution is increased. Using this technique an optical correlator has been used to process a pyramid representation of an image.[3] In a binary version of this method, input images were preprocessed with morphological filters to approximate low-pass filters to generate a binary image pyramid.[4] In addition, wavelet approximations of images at lower resolution have also been considered using this approach.[5]

The main disadvantage of the pyramid approach is the need to process an image multiple times. In addition, if multiple areas of interest exist in a low-resolution image, these areas may need to processed independently if they are not in the vicinity of each other. Therefore, valuable processing time may be spent if multiple potential objects exist in an image. What is needed is an approach where all the necessary information about an object is in a low-resolution version of an image; then, the image may be processed only once. Such a method could allow a significant decrease in processing time by, in effect processing compressed images.

In this work, we examined cross-correlation operations on a low-resolution image that was approximated by the discrete wavelet transform (DWT). After cross-correlation with a similarly processed image containing an object of interest, we synthesized the cross-correlation result to the resolution of the original image. The schematic diagram of our approach is shown in Fig. 1. Using this approach, we performed only one correlation operation and avoided passing information between levels of an image representation.

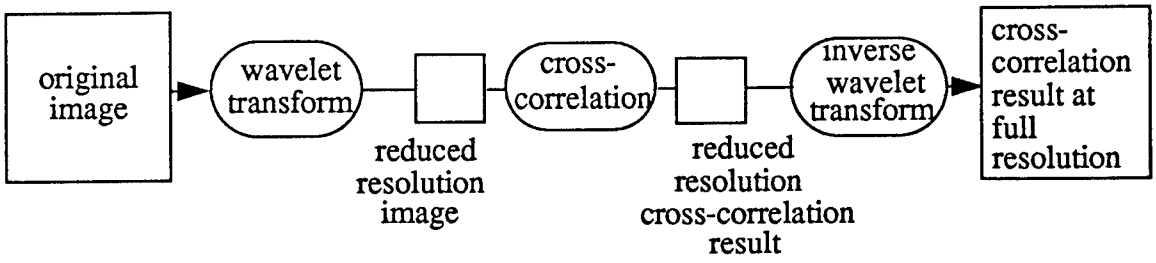

FIGURE 1. Schematic diagram of correlation process

Because we used an approximated image, the choice of filter bank for wavelet representation can be crucial. For example, in image compression applications, methods to select filter banks are often based on one or more parameters such as, maximum power,[6] minimum entropy,[7] or impulse and step response.[8] In this work, we used the latter approach in evaluating filter banks. Specifically, we used the impulse response of the system in Fig. 1, where the autocorrelation was performed on the approximated signal. We evaluated filter banks by measuring parameters such as the signal-to-noise ratio (SNR), peak-to-correlation energy (PCE), and shift variance, at the output of the system. Although we tried a limited number of filter banks, our approach provided some insight into the level of performance we can expect from our system.

In the following sections we described the multiresolution representation of an image, the approximation of an image at a lower resolution, and synthesis of a correlation result to a higher resolution using wavelet filter banks. We discussed filters for our approach and evaluated them using their impulse response. Finally, we compared auto- and cross-correlation results between images processed at full resolution and those processed at 1/4 the original resolution.

2.0 Multiresolution Processing

2.1 Multiresolution representation

The wavelet transform can be interpreted as a multiresolution representation of an image. The wavelet representation is constructed based on the difference of information at two successive res-

olutions.[9] In the following discussion, we generally discussed the wavelet representation in terms of one-dimension, but all of our equations can be easily generalized to two dimensions.

Using the wavelet representation the approximation of a signal $f(x)$ at the resolution 2^j is referred to as $A_{2^j}\{f(x)\}$ where A_{2^j} is a projection operator that approximates the function $f(x)$ and $j \leq 0$. The signal $A_1\{f(x)\}=f(x)$, is the original signal at the highest resolution, and $A_{1/2}\{f(x)\}$, $A_{1/4}\{f(x)\}$, etc. are lower resolution versions of $f(x)$. The operator A_{2^j} is an orthogonal projection on a vector space, and $A_{2^j}\{f(x)\}$ is not modified if we approximate it again at resolution 2^j. Furthermore, the approximation of a signal at a resolution 2^j contains all the necessary information to compute the signal at resolution 2^{j-1}. Finally, the approximation operation is similar at all resolutions.

2.2 Approximation of image at lower resolution

The DWT can be implemented in one dimension in an efficient manner by passing a signal through identically structured processing stages where each successive stage processes half the number of bytes as the previous stage. In this configuration, considering a discrete function $f(x)$ which has a length of N bytes, the first $N/2$ wavelet coefficients are generated at the first stage, the next $N/4$ coefficients at the next stage and so on. A schematic diagram of the DWT decomposition is shown in Fig. 2. In each processing stage, the input signal is split, then filtered by low-pass $g(n)$, and high-pass $h(n)$ filters, then downsampled. The result of the downsampled, high-pass filter operations are the wavelet coefficients at a particular scale. The detail signal $D_{2^j}\{f(x)\}$ at the resolution 2^j contains the difference of information between $A_{2^{j+1}}\{f(x)\}$ and $A_{2^j}\{f(x)\}$. The result of the downsampled, low-pass filter operations is the approximation of the input function at a particular scale, and is sent to the next processing stage. The separable two-dimensional case is a straightforward extension of this 1-D case.

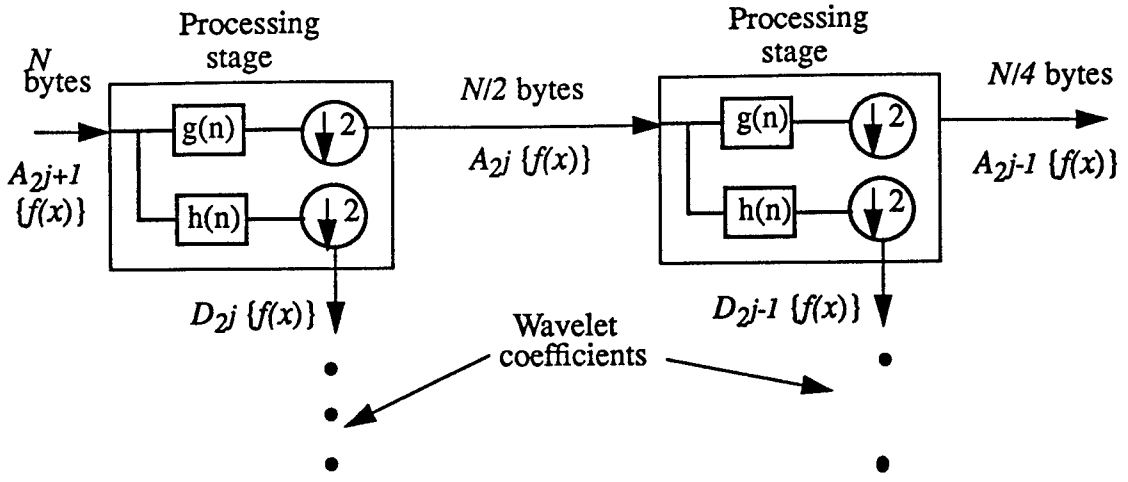

FIGURE 2. Forward DWT decomposition in 1-D.

The function used to approximate a signal at a lower resolution is called a scaling function. The approximation of a signal $f(x)$ at resolution 2^j can be viewed as a convolution between the signal $f(x)$ and a scaling function $\phi(x)$ followed by a uniform sampling at the rate of 2^j. From Fig. 2, it can be seen that a signal is approximated at a lower resolution by passing it through a series of low-pass filters and can be described in the frequency domain by,

$$\Phi(\omega) = F^{-1}\{\phi(x)\} = \prod_{k=1}^{\infty} G\left(\frac{\omega}{2^k}\right), \tag{1}$$

where $\phi(x)$ is the scaling function in the spatial domain. The approximation of a signal $f(x)$ at resolution 2^j was written as

$$A_{2^j}\{f(x)\} = \int f(x')\,\phi_{2^j}(x' - 2^{-j}x)\,dx', \tag{2}$$

where ϕ_{2^j} represents the scaling function at the resolution 2^j. In two dimensions Eq. (2) can be written as

$$A_{2^j}\{f(x,y)\} = \iint f(x',y')\,\phi_{2^j}(x'-2^{-j}x)\,\phi_{2^j}(y'-2^{-j}y)\,dx'dy', \tag{3}$$

if a separable scaling function is used. The multiresolution approximation is completely characterized by the scaling function. In addition, it is possible to chose scaling functions with good localization properties in both the frequency and input domains.

2.3 Synthesis of image to higher resolution

Similar to the forward DWT, the inverse DWT can be implemented in an efficient manner by passing a signal through identically structured processing stages where each successive stage processes twice the number of bytes as the previous stage. A schematic diagram of the inverse DWT synthesis is shown in Fig. 3.

In each processing stage the input from the previous stage and the wavelet coefficients at that stage are upsampled with zeros then passed through separate filters. The filter convolved with the wavelet coefficients is a high-pass filter represented as $\underline{h}(n)$, and the filter convolved with samples from the previous stage is represented as $\underline{g}(n)$, and are related to the filters $h(n)$ and $g(n)$ as described in the next section. The output of the filters are then summed together and sent to the next processing stage.

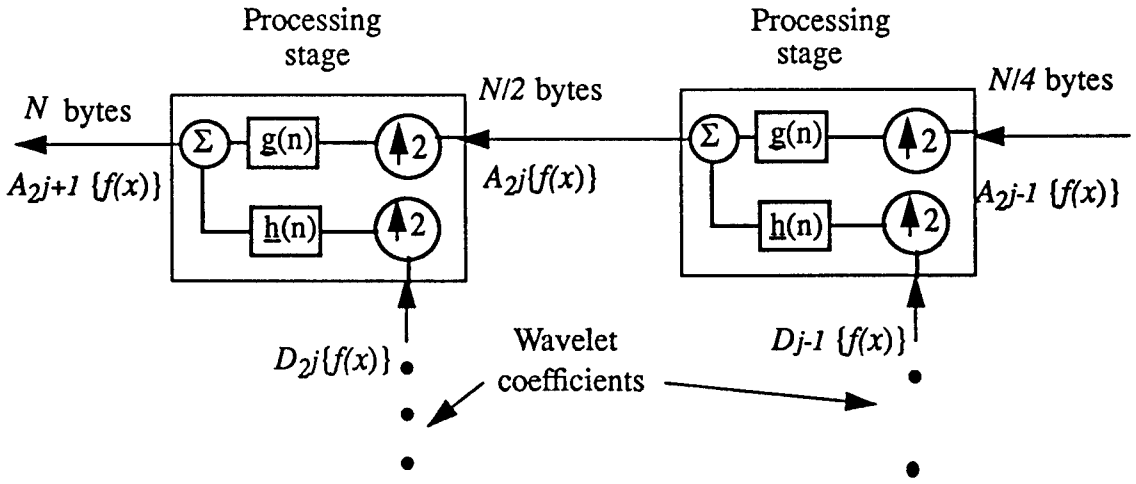

FIGURE 3. Inverse discrete WT reconstruction

To synthesize a low-resolution image to a higher resolution, an image is simply passed through the processing blocks in Fig. 3. However, in our work the wavelet coefficients were set to zero. Therefore, it is important that the reduced-resolution image contain adequate information so the higher-resolution image will be represented accurately.

2.4 Wavelet filter banks

2.4.1 Filters for orthogonal wavelets

Filters in the forward DWT that allow an orthogonal representation of a signal have mirror-image symmetry about the frequency $\omega = \pi/2$ in the frequency domain, and are referred to as quadrature mirror filters (QMFs).[10] The frequency domain relationship of QMFs is represented in Fig. 4. In the spatial domain, this can be described by

$$h(n) = (-1)^{n+1} g(p-1-n), \tag{4}$$

where p is the length of the filter. For example, if the low-pass filter had coefficients $g(n) = \{c0, c1, c2, c3\}$, then the high-pass filter would have coefficients $h(n) = \{-c3, c2, -c1, c0\}$.

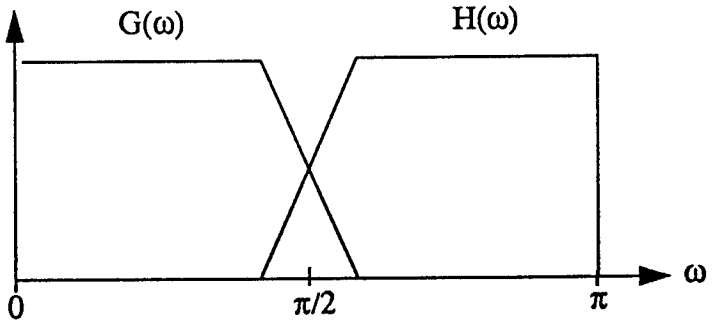

FIGURE 4. Frequency response relationship of QMFs

Aliasing resulting from downsampling in the DWT can be perfectly cancelled by properly choosing the filter coefficients in the inverse DWT.[11] For perfect reconstruction, filters used in the inverse transform, $g(n)$ and $h(n)$ must satisfy,

$$\underline{h}(n) = (-1)^n g(p-1-n) \; and, \; g(n) = \underline{g}(p-1-n). \tag{5}$$

For example, if $g(n) = \{c0, c1, c2, c3\}$, then $\underline{g}(n) = \{c3, c2, c1, c0\}$, and $\underline{h}(n) = \{c0, -c1, c2, -c3\}$.

The design of compact support, orthonormal, QMFs leads to wavelets developed by Daubechies.[12] While the QMFs have useful properties and lead to compactly supported wavelets, they cannot be finite impulse response (FIR) linear phase filters except for filters associated with the Haar wavelet.[13,14] Smith and Barnwell showed that FIR QMFs could be made nearly linear phase and called them conjugate quadrature filters (CQFs),[15] and Lawton[16] showed that FIR filters could be made to have linear phase if the filter coefficients were complex.

2.4.2 Filters for biorthogonal wavelets

The linear phase constraint corresponding to symmetrical wavelets can be maintained by relaxing the orthonormality constraint and by using biorthogonal bases.[11,17,18] The introduction of biorthogonal filters produces perfect reconstruction-FIR linear phase filters at the expense of having different but related high- and low-pass filters (and wavelets) in the forward and inverse DWT. Biorthogonal wavelets can be shown to have filters that obey,

$$\underline{h}(n) = (-1)^{n+1} g(p-1-n) \; and, \; \underline{g}(n) = (-1)^{n+1} h(p-1-n). \tag{6}$$

In other words, the low-pass filter in the forward transform and the high-pass filter in the inverse transform form a QMF. And, the low-pass filter in the inverse transform and the high-pass filter in the forward transform form a QMF. But the low- and high-pass filters in the forward or reverse transform do not form a QMF.

Like orthogonal wavelets, biorthogonal wavelet coefficients are produced from a combination of high- and low-pass filtering. The difference between the orthogonal and biorthogonal case is that the scaling functions and wavelets in the inverse and forward transform are different. The scaling functions are related to the low-pass filters of the forward and inverse DWT in the frequency domain by,

$$\Phi(\omega) = \prod_{k=1}^{\infty} G\left(\frac{\omega}{2^k}\right) \; and \; \underline{\Phi}(\omega) = \prod_{k=1}^{\infty} \underline{G}\left(\frac{\omega}{2^k}\right) , \tag{7}$$

where $\Phi(\omega)$, and $\underline{\Phi}(\omega)$ are the Fourier transforms of the scaling functions associated with the forward and inverse DWT respectively, and $\underline{\phi}(x)$ is the inverse Fourier transform of $\underline{\Phi}(\omega)$.

3.0 Selection Of Filters For Wavelet Representation

Because we used an approximated image for further processing, the choice of filter bank for wavelet representation can be crucial. We evaluated filters using a similar technique as in Ref. 8 to select filters for image compression. There, impulse and step responses of multiple processing stages were measured. Parameters such as sidelobe strength, and minimization of shift variance were made on many analysis-synthesis sets of wavelet filters. Using this technique wavelet filters for image compression were selected based on traditional measurements rather than an ad hoc method. Although we tried a limited number of filter banks, our approach provided some insight into the level of performance we can expect from our analysis-synthesis system.

We used the impulse response of the system in Fig. 1 to evaluate wavelet filters. The square of the autocorrelation was used as the input to the inverse DWT to reflect the optical application; in an optical correlator, it is the square of the correlation response that is measured. We evaluated filter banks by measuring parameters such as the signal-to-noise ratio (SNR), peak-to-correlation energy (PCE), and shift variance, at the output of the system.

We evaluated wavelet filters in 1-D using a 256-byte length vector with an impulse as the input signal. The input vector was approximated at 1/4 the original resolution using the wavelet transform with a 64-byte length vector. Then, we performed the autocorrelation of the 64 length approximation of an impulse using a binary phase-only filter (BPOF). In our BPOF, the amplitude was set to unity, and the phase value was set to ± 1 depending on the sign of the real part of the approximated impulse's Fourier transform. Following the autocorrelation, we synthesized the autocorrelation result to a 256-byte length vector using the inverse wavelet transform. Because the wavelet transform is not shift invariant, we produced all impulse responses and calculated the total mean-squared error by summing the variances of the responses at each point.

We used a limited number of wavelet filters in our evaluation to give insight into our approach, Specifically, we used Daubechies biorthogonal symmetric (DBS) wavelets[19] which produced the results in Table 1.

TABLE 1. Wavelet Filter Parameters for Impulse Response using a BPOF

Wavelet	Square of Correlation Height (avg.)	SNR	PCE	MSE of shift variance x 10^{-4}
DBS 1,1	45.6	0.84	13.5	1.51
DBS 1,3	56.0	0.88	15.8	1.62
DBS 1,5	83.1	1.30	15.8	1.61
DBS 2,2	240	3.88	13.7	8.00
DBS 2,4	35.4	0.55	13.5	2.76
DBS 2,6	130	2.17	13.5	2.60
DBS 2,8	55.2	0.86	14.6	1.62
DBS 3,1	477	7.46	14.0	20.5
DBS 3,3	193	3.02	14.1	5.01
DBS 3,5	118	1.84	15.2	2.69
DBS 3,7	194	3.04	13.4	5.25
DBS 3,9	104	1.63	15.7	4.62
DBS 4,4	26.2	0.41	12.8	1.38
DBS 5,5	38.2	0.60	15.5	1.27

From the data in Table 1, the impulse response due to different wavelets varied considerably for some parameters, but not for others. For example, the average of the squares of the autocorrelation heights due to the fourteen wavelet filters varied from a maximum of 477 to a minimum of 26.2, for a ratio of 18.2. The SNR varied by the same ratio. The PCE and MSE of the shift variance had ratios of maximum to minimum of 1.23, and 16.1 respectively.

The DBS(3,1) wavelet filters clearly produced the largest values for the autocorrelation height and SNR. We didn't consider the PCE values in filter selection because they were similar. Although the shift invariance was significantly higher for the DBS(3,1) wavelet filters than others we still considered it for additional experiments because the SNR was so high.

To better understand the effect of the DBS(3,1) wavelet filters, we examined the frequency response of the system in Fig. 1 when an impulse was used as an input. The impulse was autocorrelated with a BPOF at 64-byte length, then squared before being synthesized to a 256-byte length. The magnitude of the frequency response of the impulse response of the system is shown in Fig. 5. It can be seen that significant attenuation of the higher frequencies occurred.

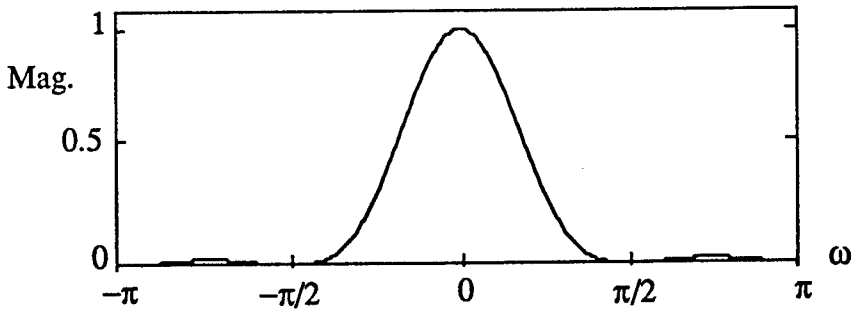

FIGURE 5. Impulse response of DBS(3,1) wavelet filters at output of system in Fig. 1, in frequency domain

4.0 Experimental Results

We compared correlation results performed on 256 x 256 pixel images at full resolution, with those performed on 64 x 64 images approximated and synthesized with the DBS(3,1) wavelet. Because the wavelet transform is not shift invariant, there should be 16 different responses. These come from product of two levels of decomposition ([2 responses] $^{2\ \text{levels}}$), and two dimensions. Had there been three levels of decomposition, there would have been 64 different responses. We considered the image in Fig. 6 for autocorrelation experiments and tabulated the results in Table 2. We only showed the results for one relative position of the input and output images, but the results are similar for other relative positions.

Although the correlation height decreased when the image was processed at a lower resolution, the SNR increased, and the result appeared visually useful for object identification. The decrease in correlation height and increase in SNR can be explained by frequencies contributing to noise with little signal being attenuated.[19] Although the SNR has significantly increased, it still

is below the maximum obtained with a matched filter at full resolution which is 86.0 db. The correlation height decrease was due to the attenuation of energy as indicated in Fig. 5. The autocorrelation response of full and 1/4 resolution processing are shown in Figs. 7(a) and (b) respectively. Note that both results are at 256 x 256 pixel resolution.

TABLE 2. Comparison of Results for 256 x 256, an 64 x 64 Pixel Correlations

	256 x 256 resolution	64 x 64 resolution
Correlation height	57.5 db	40.5 db
SNR	9.3 db	53.6 db
PCE	1.64	0.03
Discrimination	0.89	0.13

The PCE is a measure of sharpness of the correlation peak and is the ratio of the energy in the correlation peak to the energy in the input image.[20] The PCE decreased when images were approximated at a lower resolution before for autocorrelation. This was due to the decrease in the correlation peak, which was due to the attenuation of energy at some spatial frequencies.

We also compared the discrimination between two similar objects shown in Figs. 6 and 8 respectively. We calculated the discrimination between the two figures as the difference between the correlation peaks obtained with Figs. 6 and 8, divided by the correlation peak obtained with Fig. 6. In all cases, we used the BPOF of the object in Fig. 6. The discrimination decreased when images where processed at a lower resolution.

To gain insight into whether the discrimination is useful for pattern recognition, we then used an image with both types of objects present. We used the image in Fig. 9 and cross-correlated it with a BPOF made from the image in Fig. 6. Figure 9 shows three objects, two of which are in the same class. Fig. 10(a) and (b) shows the resulting cross-correlation when processed at full resolution and 1/4 resolution respectively. One performance parameter we used was the signal-to-clutter ratio (S/C), which is the ratio of the lowest correlation peak of an in-class object, to the highest peak of an out-of-class object. The other measure was the spread of the in-class correlation peaks, which was the ratio of the maximum to minimum correlation peaks of the in-class objects. For the

image processed at full resolution, the S/C was 5.2db, and the in-class spread was 0.12db. When the image was processed at 1/4 resolution, the in-class spread increased slightly to 0.17db, and the S/C decreased to 2.3db indicating a decrease in discrimination ability. In addition, the cross-correlation with the background significantly increased. The background, primarily the region on the left in Fig. 9, produced a larger correlation than the out-of-class plane. If the background was taken into consideration, then the S/C had decreased to 0.8db.

5.0 Discussion and conclusion

We showed that we could recognize objects at 1/4 resolution using the wavelet representation and BPOF correlation filters. Using our approach, we avoided cross-correlating an image multiple times and passing information between levels of an image representation. In our experiments, the SNR increased, while discrimination and PCE decreased for the wavelet filters chosen. Although discrimination decreased, it appeared that the results were useful for object recognition. Different wavelet filters gave different autocorrelation and SNR values for their impulse response; therefore, the choice of wavelet filters could be significant in processing an image at lower resolutions. Although this study gives insight into the performance that may be expected when performing pattern recognition as described here, we need to theoretically establish the potential of this approach.

6.0 References

[1] A. D. Gross, and A. Rosenfeld, "Multiresolution object detection and delineation," *Computer Graphics & Image Proc.* 39, 102-115 (1987)

[2] P. J. Burt, in *Multi-resolution Image Processing and Analysis*, A. Rosenfeld, ed., Chap. 2, Springer-Verlag: Berlin (1984)

[3] S. P. Kozaitis, Z. Saquib, R. H. Cofer, and W. E. Foor, "Multi-resolution template matching using an optical correlator," in *Hybrid Image and Signal Processing III*, D. Casasent, and A. Tescher, Eds., Proc. SPIE 1702-15 (1992)

[4] S. P. Kozaitis, and W. E. Foor, "Binary optical correlation using pyramidal processing," *Optical Engineering* 33(6), 1838-1844 (1994)

[5] S. P. Kozaitis, and R. H. Cofer, "Multiresolution optical correlation using the wavelet transform," in *Optical Pattern Recognition VI*, Proc. SPIE 2490-19 (1995)

[6] M. Unser, "On the optimality of ideal filters for pyramid and wavelet signal approximation," *IEEE Trans. Signal Processing*, vol.41(12), 3591-3596 (1993)

[7] Y. Zhang, and J. S. Baras, "Optimal wavelet basis selection for signal representation," in *Wavelet Applications*, H. Szu, Ed., Proc. SPIE 2242, 200-211 (1994)

[8] J. D. Villasenor, B. Belzer, and J. Liao, "Wavelet filter evaluation for image compression," *IEEE Trans. Image Processing*, vol.4(8), 1053-1060 (1995)

[9] S. G. Mallat, "A theory for multiresolution signal decomposition: the wavelet representation," *IEEE Trans. on Pat. Anal. Mach. Int.* 11(7), 674-693 (1989)

[10] J. G. Proakis, C. M. Rader, F. Ling, and C. L. Nikias, "Advanced signal processing," Macmillan: New York (1992)

[11] R. K. Young, "Wavelet theory and its applications", Kluwer Academic Publishers: Boston (1993)

[12] I. Daubechies, "Orthonormal bases of compactly supported wavelets, *Comm. Pure Appl. Math.*, vol. 41, 909-996 (1988)

[13] A. Cohen, I. Daubechies, and J.-C. Feauveau, "Biorthogonal bases of compactly supported wavelets," *Comm. in Pure and Appl. Math.*, vol. 45, 485-560 (1992)

[14] M. Vetterli, and C. Herley, "Wavelets and filter banks: Theory and design," *IEEE Trans. Signal Processing*, vol. 40(9), 2207-2232 (1992)

[15] M. J. T. Smith, and T. P. Barnwell III, "Exact reconstruction techniques for tree-structured subband coders," *IEEE Trans. ASSP*, Vol. ASSSP-34(3), 434-441 (1986)

[16] W. Lawton, "Application of complex-valued wavelet transforms to subband decomposition," *IEEE Trans. Signal Processing*, (1993)

[17] A. Cohen, "Biorthogonal wavelets and dual filters," in *Wavelets in Image Communication*, M. Barlaud, Ed., Elsiever Science: Amsterdam, 1-26 (1994)

[18] M. Antonini, T. Gaidon, P. Mathieu, and M. Barlaud, "Wavelet transform and image coding," in *Wavelets in Image Communication*, M. Barlaud, Ed., Elsiever Science: Amsterdam, 65-188 (1994)

[19] B. V. K. Vijaya Kumar, and R. D. Juday, "Design of phase-only, binary phase-only, and complex ternary matched filters with increased signal-to-noise ratios for colored noise," *Opt. Lett.* 16(13), 1025-1027 (1991)

[20] B. V. K. Vijaya Kumar, and L. Hasselbrook, "Performance measures for correlation filters," *Applied Optics* 29(20), 2997-3006 (1990)

FIGURE 6. 256 x 256 pixel image used in autocorrelation experiments.

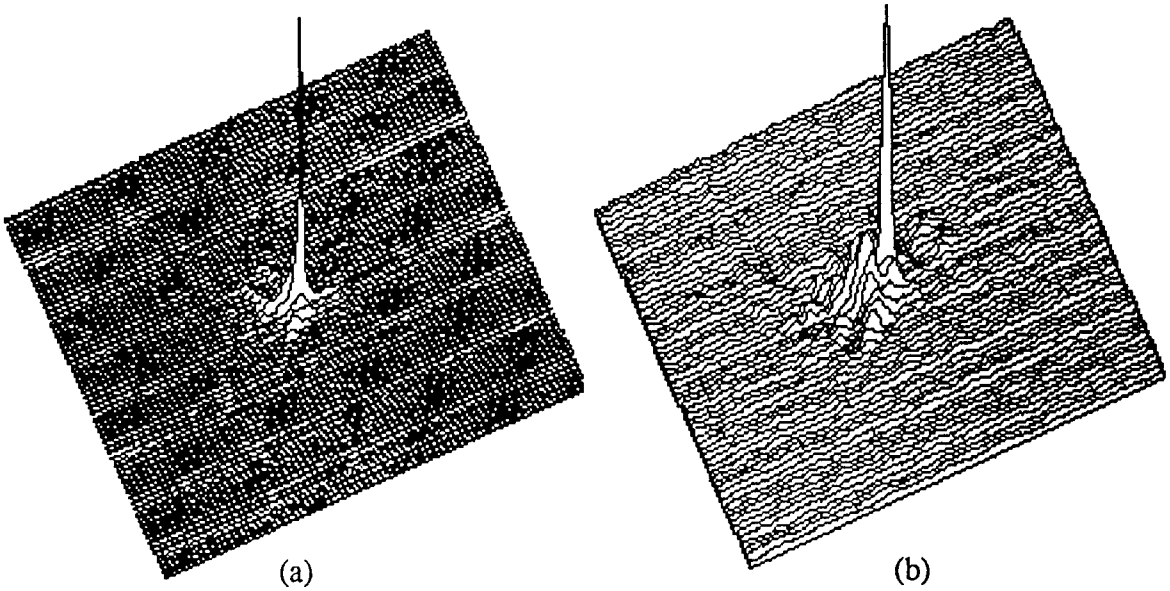

FIGURE 7. Autocorrelation of image in Fig. 6 using a BPOF processed at (a) full resolution (b) 1/4 resolution

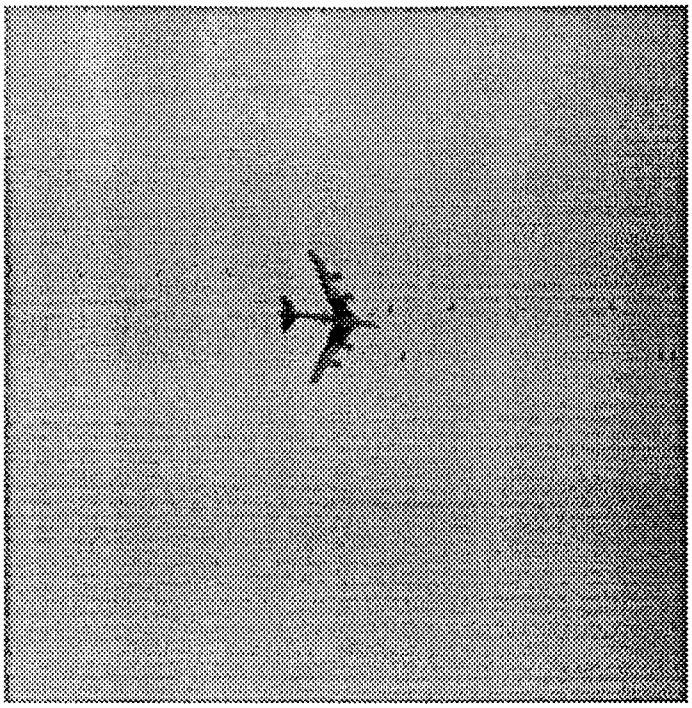

FIGURE 8. 256 x256 pixel image used in discrimination experiments.

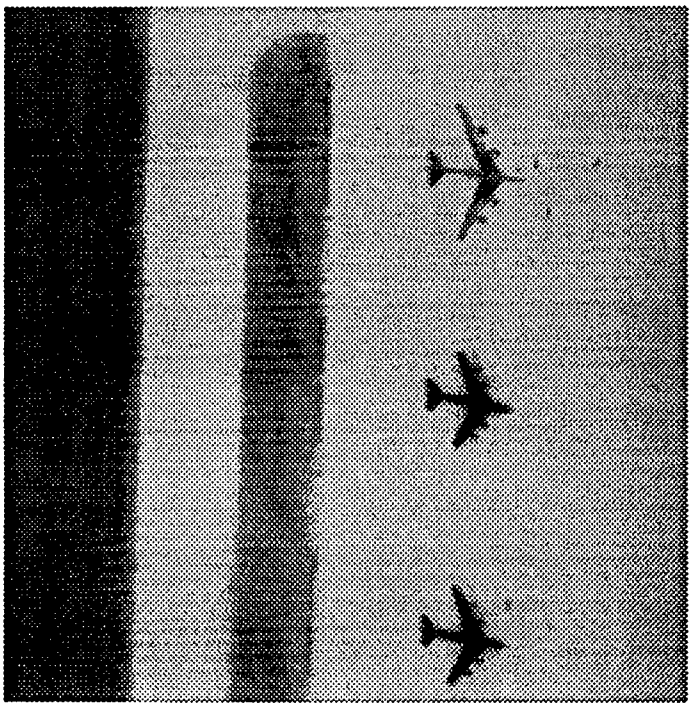

FIGURE 9. 256 x 256 pixel image used in cross-correlation experiments.

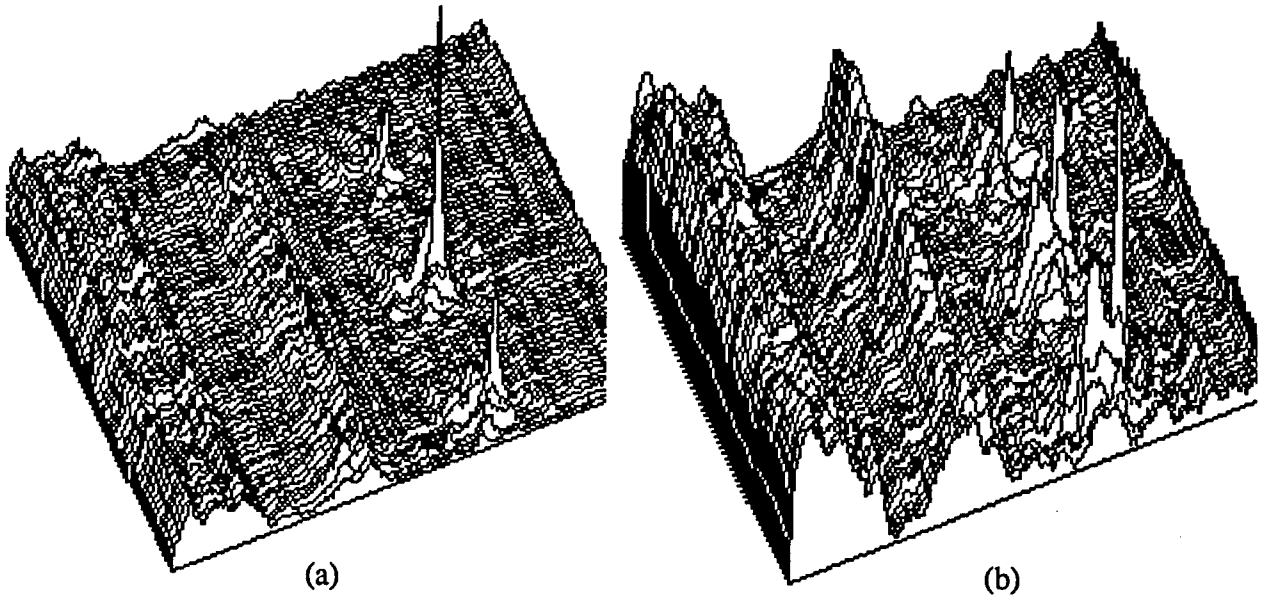

FIGURE 10. Cross-correlation of image in Fig. 9 with image in Fig. 6 using a BPOF processed at (a) full resolution (b) 1/4 resolution

*U.S. GOVERNMENT PRINTING OFFICE: 1996-710-126-47009

MISSION

OF

ROME LABORATORY

Mission. The mission of Rome Laboratory is to advance the science and technologies of command, control, communications and intelligence and to transition them into systems to meet customer needs. To achieve this, Rome Lab:

a. Conducts vigorous research, development and test programs in all applicable technologies;

b. Transitions technology to current and future systems to improve operational capability, readiness, and supportability;

c. Provides a full range of technical support to Air Force Materiel Command product centers and other Air Force organizations;

d. Promotes transfer of technology to the private sector;

e. Maintains leading edge technological expertise in the areas of surveillance, communications, command and control, intelligence, reliability science, electro-magnetic technology, photonics, signal processing, and computational science.

The thrust areas of technical competence include: Surveillance, Communications, Command and Control, Intelligence, Signal Processing, Computer Science and Technology, Electromagnetic Technology, Photonics and Reliability Sciences.